Depth modelling and imaging of the 4D seismic survey of the Basso Livenza area (NE Italy)

S. Picotti, M. Giustiniani, F. Accaino and U. Tinivella

Istituto Nazionale di Oceanografia e di Geofisica Sperimentale , Trieste, Italy

(Received: November 2, 2007; accepted: December 5, 2007)

ABSTRACT We apply a modelling and in-depth imaging procedure to the 4D high-resolution seismic data acquired in Basso Livenza (Friuli-Venezia Giulia, NE Italy), in order to characterize an important multilayered aquifer. The survey consists in four 3D seismic cubes, acquired in two different zones and periods (March and July). This system is made up of an unconfined layer and, at increasing depths, of several confined aquifers of variable thickness and hydraulic permeability, mainly consisting of sandy/gravel material. In particular, two saturated bodies, located at about a 30 m and a 180 m depth respectively, are known very well from the well stratigraphies of the aqueduct of Basso Livenza. The purpose of this work is to build a 3D image of the aquifer, in order to extend the well information to the surrounding area, and to investigate the difference in the P-wave velocity of the saturated layers between the two periods. In the 3D cubes, two high-velocity layers were identified at about 270 m and 480 m respectively, which correspond in the stratigraphy of a recent well to new, deeper aquifers. However, considering a velocity error of about 5%, the seismic method cannot detect any difference in the overpressure condition of the aquifers between the two periods.

1. Introduction

During the winter of 2005, three 2D high-resolution seismic lines were acquired near Torrate (Friuli-Venezia Giulia, north-eastern Italy), in an area with several catchment wells of the aqueduct of Basso Livenza (ABL). As described in Giustiniani *et al*. (2009), this 2D seismic survey allowed us to determine a preliminary subsurface geometry of the analyzed aquifer system and to optimize a later 4D survey. Successively, four 3D seismic cubes were acquired in two different seasons and in two different areas (Fig. 1). The smaller, yellow, 3D cube acquired in March 2006 is called cube 1, while the data acquired in July is hereafter called cube 2. The bigger 3D cube, (Fig. 1) is named cube 3 when referred to the data acquired in March, and cube 4 when referred to the data acquired in July.

The data were processed (Giustiniani *et al.*, 2009), using a commercial software, in order to enhance the signal-to-noise ratio and to increase the vertical resolution by adopting the "true-amplitude" approach. This procedure allowed a successive Amplitude Versus Offset (AVO) analysis (Yilmaz, 2001), described in Tinivella *et al*. (2009).

The seismic data were then analyzed by adopting an iterative modelling and in-depth imaging procedure, with the main purpose of building a 3D image of the aquifer. The technique described in this work consists in an iterative updating procedure for refining and improving an initial

model in depth, involving pre-stack depth migration, residual move-out analysis and seismic reflection tomography. The initial model is generally deduced from geological field surveys, or derived by adopting other techniques. In our case, we used a velocity-depth model derived from the interpolation of the velocity sections relative to the preliminary 2D seismic survey. At every iteration, both velocity and reflector geometries are updated, until the two sets of parameters reach a good degree of stability and consistency.

2. Overview of the imaging approach

Seismic representation of an Earth model in depth is usually described by two sets of parameters: layer velocities and depth of interfaces. Difficulties in estimating these parameters with a required level of accuracy make the Earth model estimation a challenging task for seismic exploration. The concept of a depth model, by which the Earth velocity field can be constructed and optimised is very useful in seismic exploration. Subsurface imaging is finally realized by pre-stack depth migration, that converts the seismic data into an image of the Earth by using the velocity field. The more reliable the velocity field we supplied to the migration, the more realistic is the imaging. Nearly all of the practical modelling methods are based on ray theory, and more specifically, on the inversion of seismic traveltimes. In the following section, we will describe the procedure adopted in this work in detail.

2.1. The residual move-out analysis

Residual move-out analysis is a velocity analysis performed after applying an imperfect initial velocity function to the data, in order to find the remaining error in the velocity field. If the initial velocity field has been estimated with sufficient accuracy, then the common image gathers (CIGs), derived from pre-stack depth migration using this model, should exhibit flat events. Any errors in layer velocities and/or reflector geometry, on the other hand, should give rise to a residual move-out along those events on the CIGs, which are non-flat in thise case. In other words, the degree of non-flatness of the reflection events on the CIGs is a measurement of the error in the model, and residual move-out analysis identifies the correction required to flatten reflection events (Yilmaz, 2001).

The residual move-out is a measurement of non-flatness, defined by the difference between the location of the reflection event on the near and far offset traces. Generally, a fixed offset value, known as “reference offset”, is used for far offset. As shown in Fig. 2a, a positive residual indicates that the local velocity used for the depth migration is too high, while a negative residual is associated with a too low velocity.

The method of performing residual move-out analysis utilises semblance sections, obtained by scanning various residuals, and is similar to that of standard stacking velocity analysis. This method, implemented in many commercial software packages, computes a semblance value for every residual and creates a semblance section. A vertical function that represents the depth-dependent residual move-out can be picked from the semblance sections. This function can then be used to correct for the residual move-out, and so improve the velocity field in order to obtain a better depth-migrated section.

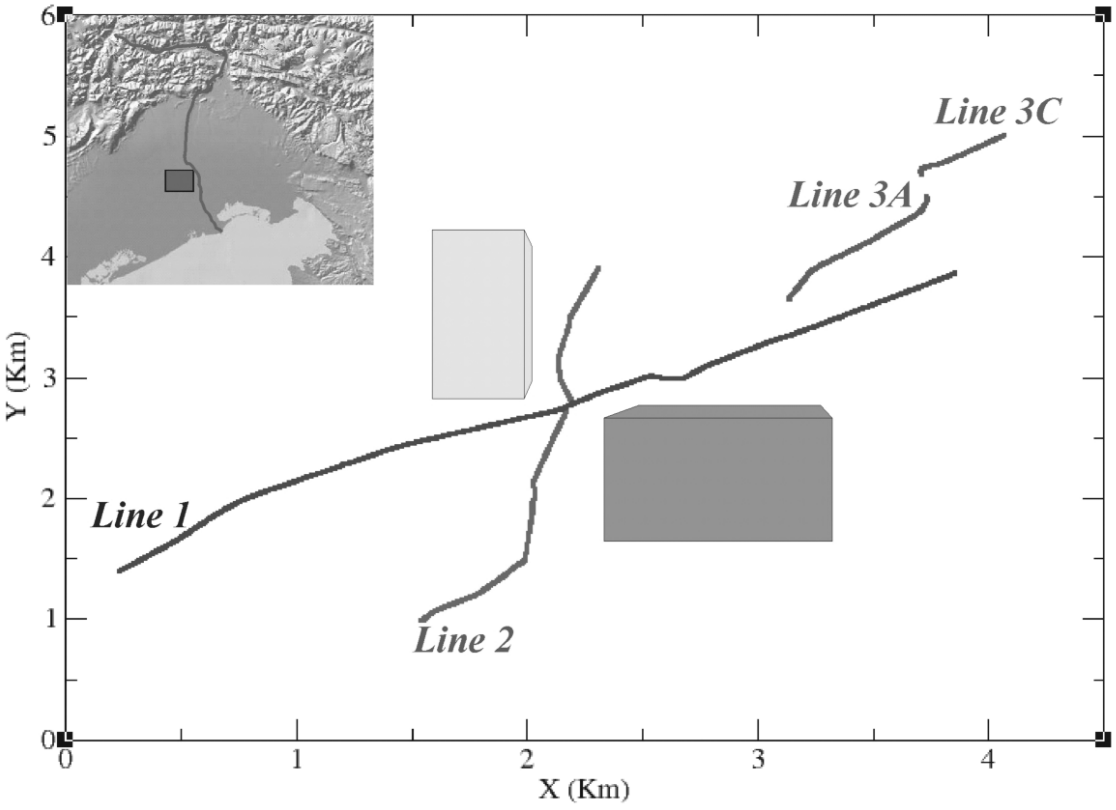

Fig. 1 - Location map of the three 2D seismic lines and the two 3D seismic cubes.

2.2. Horizon-Based Tomography

The tomography of depth migrated gathers is a method for refining the velocity-depth model when pre-stack depth migration is performed with an incorrect velocity field. The degree of non-flatness of the reflection events on the CIGs is a measurement of the error in the model. Therefore, since residual move-out is a measurement of non-flatness, Horizon-Based Tomography (HBT) uses residuals as input and attempts to find an alternative model which will minimise the error; i.e. produce flatter gathers (Yilmaz, 2001).

The first step in HBT is to scale the residuals to time using the initial model. A difference in time Δt, obtained scaling a specific residual, represents an error in travel-time measured at a specific Common Mid Point (CMP) location. The tomographic approach attributes the value of Δt to an accumulation of errors Δt_i within each layer where the ray has travelled. In other words, the error Δt can be the result of an error in the model at any point along the ray. Moreover, an error in the model can be an error in velocity Δv_i or depth Δz_i. So, the objective is to obtain Δt_i, the error in travel-time within each layer, and derive the error in velocity, Δv_i, and the error in depth Δz_i from Δt_i.

A basic part of the tomography algorithm is the Common Reflection Point (CRP) ray tracing. One equation is written for each k-ray:

$$\Delta t_k = \sum_{i=1}^{n} \Delta t_{ki} \tag{1}$$

The resulting system of equation can be written in the matrix form:

$$\Delta t = L \Delta p \tag{2}$$

where Δt denotes the column vector that represents the residual move-out times measured from the image gathers, and Δp is the tomographic update column vector that comprises the changes in the slowness and depths to layer boundaries. L is a sparse matrix: its elements are exspressed in terms of slowness and depth parameters associated with the initial model.

The system of equations is then solved using least-squares and the tomographic update Δp is given by the Generalised Linear Inversion (GLI) solution:

$$\Delta p = (L^T L)^{-1} L^T \Delta t \tag{3}$$

where T denotes matrix transposition.

2.3. Earth modelling in depth

Consider an initial model, made up of horizontal layers with laterally invariant velocities, or partially refined adopting other techniques. We shall make an attempt to update this initial estimate using the modelling procedure described by the flow-chart shown in Fig. 2b. As you can see, this is an iterative updating procedure involving pre-stack depth migration, residual move-out analysis and seismic reflection tomography. We can summarise it as follows:

1. Generate a set of CIGs from pre-stack depth migration using the velocity field derived from the initial model.
2. If the CIGs exhibit flat events, then the model is good and the procedure stops giving the final model and the imaging performed by the pre-stack depth migration. If the events are not flat, the model is not yet sufficiently accurate, and the procedure goes on.
3. Compute the horizon-consistent residual move-out for all offsets along events on CIGs that corresponds to layer boundaries included in the model, obtaining the semblance sections.
4. Pick on the residual move-out profiles for all the horizons by tracking the semblance peaks.
5. Build the travel-time error vector Δt using the picked residual move-out in depth.
6. Define the initial model by a set of slowness and depth parameters and construct the coefficient matrix L in Eq. (2).
7. Estimate the change in the parameters vector Δp, by way of the GLI solution given by Eq. (3).
8. Update the parameter vector $p+\Delta p$. By combining the update interval velocity profiles with the new depth horizons, we obtain the updated model.

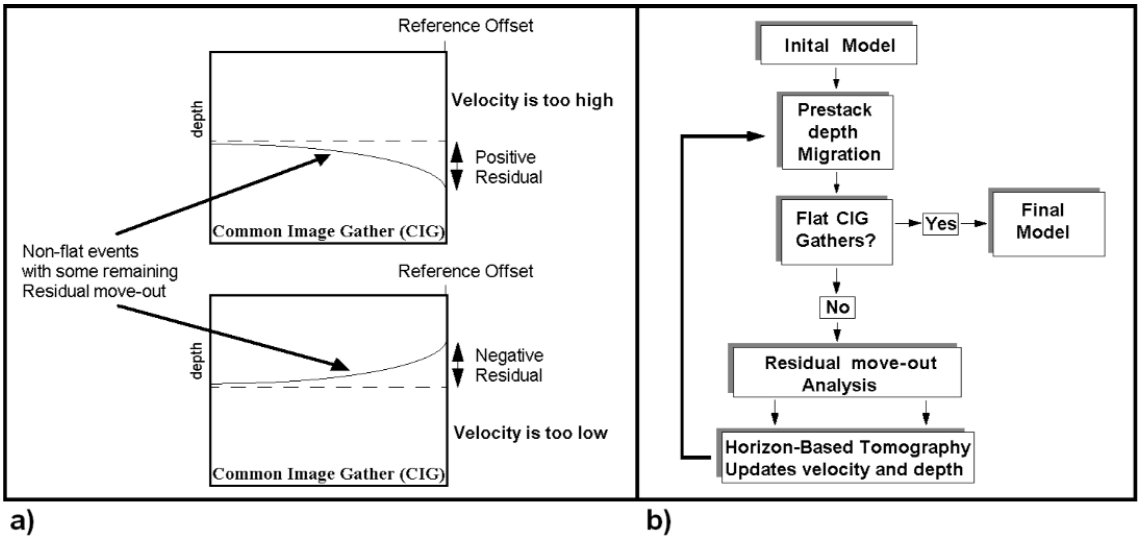

Fig. 2 - The concept of residual move-out on a CIG (a) and flow-chart of a typical modelling in depth procedure (b).

9. Extract the velocity field from the new model and perform the pre-stack depth migration.
10. Return to point 2.

This procedure goes on until the quality of the pre-stack depth migration is not sufficient. Generally, this point is reached when the events on the CIGs become flat (Yilmaz, 2001).

3. Modelling and imaging of the data

As described previously, after a preliminary processing of the data (Giustiniani *et al*., 2009), we proceeded with the modelling and imaging phase.

3.1. Construction of the initial model

The 3D imaging was carried out in two sessions: in the first we reached a first estimation of the velocity-depth model by interpolating the 2D sections obtained using a tomographic software realised by an OGS research team (Vesnaver *et al*., 1999; Rossi *et al.*, 2001; Giustiniani *et al*., 2009). In the second we refined the model and performed the 3D pre-stack depth migration using a modelling commercial package. According to the modelling procedure shown in Fig. 2b, we used the initial velocity field to perform a first pre-stack depth migration of the seismic data acquired in March (cube 1). The result shows that the image quality is not good yet, because the seismic energy is not well focused. This is due to the fact that the CIGs derived from pre-stack depth migration exhibit non-flat events. Since the geometry of the interfaces is not consistent with the reflectors on the migrated section, a reinterpretation of the model is necessary. The adopted software provides an Interpretation Module by which it is possible to pick, on longitudinal or transversal sections of the migrated cube, a new geometry of the interfaces, in order to better fit the reflectors on the migrated data.

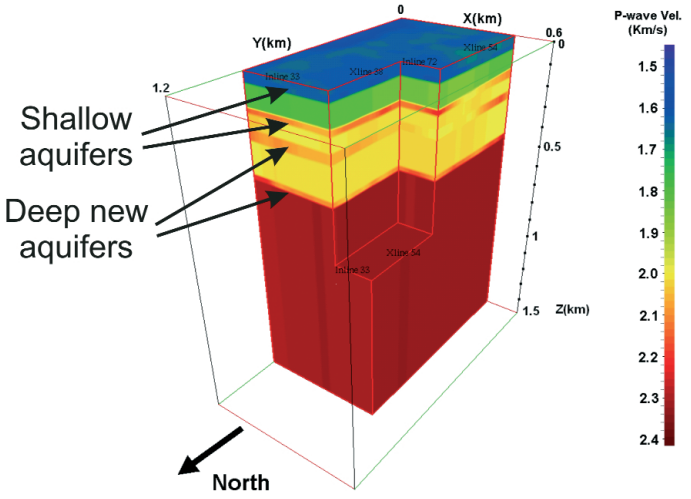

Fig. 3 - The final tomographic velocity-depth model for cube 1.

3.2. Refinement of the model

As previously explained, residual move-out can be determined and used for model updating. We carried out a residual move-out analysis, for all the horizons, by picking the coherences on the semblance profiles. For each semblance panel picked, a residual move-out function is defined. Obviously, it is not necessary to pick all the CIGs, because the residual move-out functions can be interpolated, in order to make a residual move-out map for each horizon. These maps are created by combining the residuals with the depth horizons. The residual maps and the interval velocity sections extracted from the initial model for each depth horizon, are the input data for the tomographic update.

Following the update, the new model needs to be checked for consistency with the input seismic data (Yilmaz, 2001). According to the modelling flow-chart in Fig. 2b, a second pre-stack depth migration is performed, using the velocity field derived from the new model. The main consistency checks are the following:

1. Overlay the depth horizons from the updated model onto the image section derived from pre-stack depth migration and note if they coincide with the reflectors associated with the layer boundaries included in the model.
2. Compute the residual move-out semblance spectra from the image gathers at selected locations after the model update and compare them with those before the update.

The residual move-out analysis of image gathers and the update of velocity-depth model should be performed iteratively until the velocity-depth model and the depth image are consistent. Irrespective of the strategy followed to derive the initial model, the result of modelling updating needs to be verified for consistency with the input seismic data and examined for any remaining residual move-outs to decide whether or not to continue with the iterations of the tomographic update (Yilmaz, 2001). After the third tomographic update, the events on the CIGs are nearly flat and the depth horizons associated with the updated model, when superimposed on

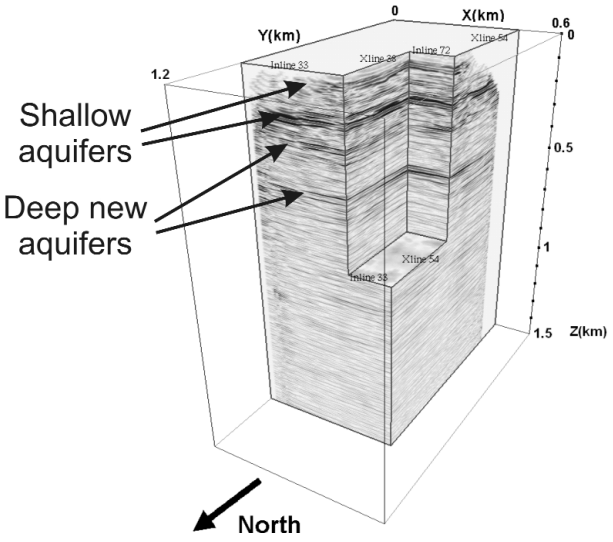

Fig. 4 - 3D pre-stack depth migration of cube 1 using the final velocity model (Fig. 3).

the image section, coincide with the reflectors that correspond to the layer boundaries. This means that the model reached a good accuracy.

4. Migration of the data

4.1. The small cubes

In Fig. 3, the final velocity cube for the data acquired in March (cube 1) is shown. With respect to the first model estimation, the vertical resolution is increased and other two, high velocity layers were identified, at about 270 m and 480 m, respectively, which could be associated to new deeper aquifers. Fig. 4 shows the final migrated cube 1: we notice that the seismic energy is well focused and two new reflections that before were not visible before appeared under a depth of 250 m. The cube is sectioned to show the good lateral continuity of the reflectors.

We adopted the same refinement procedure described above (Fig. 2b) to obtain the final velocity cube for the seismic data acquired in July (cube 2), whose figure we omitted because it is very similar to those of Fig. 3. The resulting migrated cube is shown in Fig. 5.

4.2. The large cubes

Finally, we adopted the same refinement procedure to perform the depth imaging of the large cubes (cube 3 and cube 4). In Fig. 6, the final velocity cube for the data acquired in March (cube 3) is shown, while the resulting migrated cube is shown in Fig. 7. With respect to the small cubes, we notice that the resolution and lateral continuity is much better. This is because, the coverage of the large cubes is higher with respect to the small cubes. As you can see, the two new reflections identified in the small cubes at about 270 m and 480 m are better visualized here. Moreover, other two layers were identified and picked between the two shallow aquifers.

Fig. 8 shows the final migrated cube of the data acquired in June (cube 4). The corresponding velocity cube is omitted because it is very similar to those of Fig. 6.

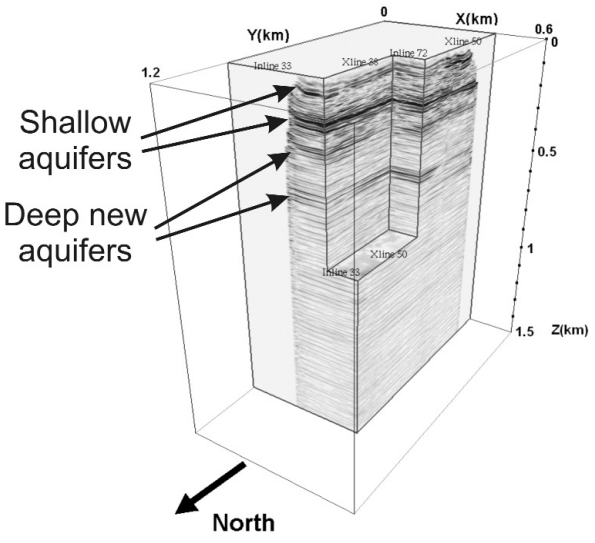

Fig. 5 - 3D pre-stack depth migration of cube 2 using the final velocity model.

In the chaircut of the migrated cube 3 (Fig. 7) a lateral amplitude inversion in the shallow layers is evidenced (with a circle). In the migrated cube 4 (Fig. 8) this is not evident, but the coverage in the same zone is very low. This lateral amplitude inversion may be due to lateral changes in the lithology or to a fault.

5. Seismic and well data correlation

After the seismic data analysis, integrated by other geophysical (i.e., TDM and geoelectrical)

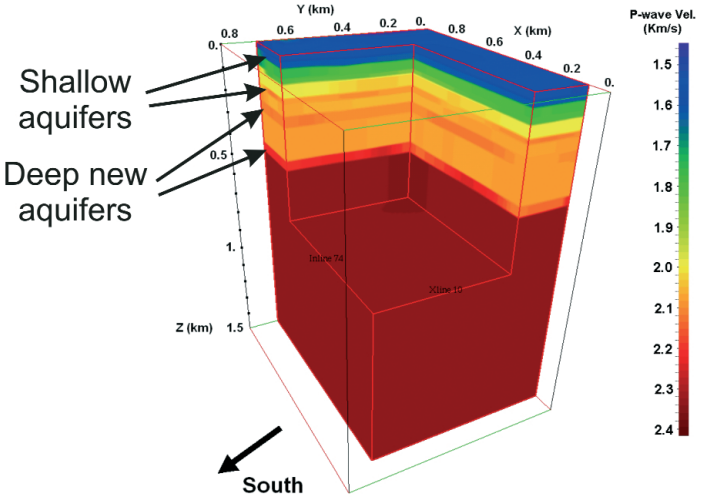

Fig. 6 - The final tomographic velocity-depth model for cube 3.

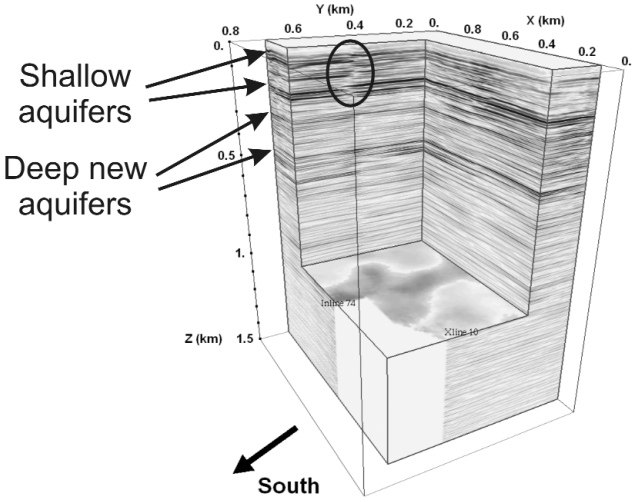

Fig. 7 - 3D pre-stack depth migration of cube 3 using the final velocity model (Fig. 6).

data a new 510 m deep well, drilled by ABL, considering the results of the seismic survey, allowed us to check the real consistency of the 3D pre-stack depth migration and the final velocity field. Fig. 9 shows a transversal depth section of cube 2, overlapped to the corresponding interval velocity section, together with the well stratigraphy and the down-hole velocity log. There is an excellent correspondence between the horizons picked on the migrated section and the main discontinuities reported in the well stratigraphy, except only for some small discrepancies, which could be due to the distance of the well from the survey area (about 200 m). As you can see, the two high velocity layers at about 270 m and 480 m correspond to other two new deeper aquifers in the well stratigraphy. Moreover, the Fig. 9 shows that there is a good correlation between the

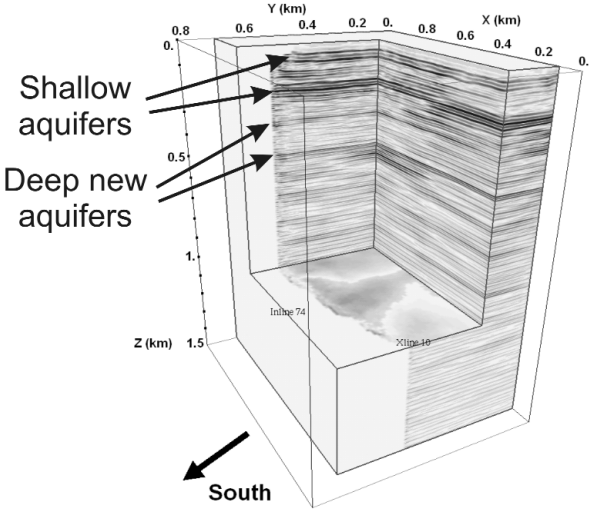

Fig. 8 - 3D pre-stack depth migration of cube 4 using the final velocity model.

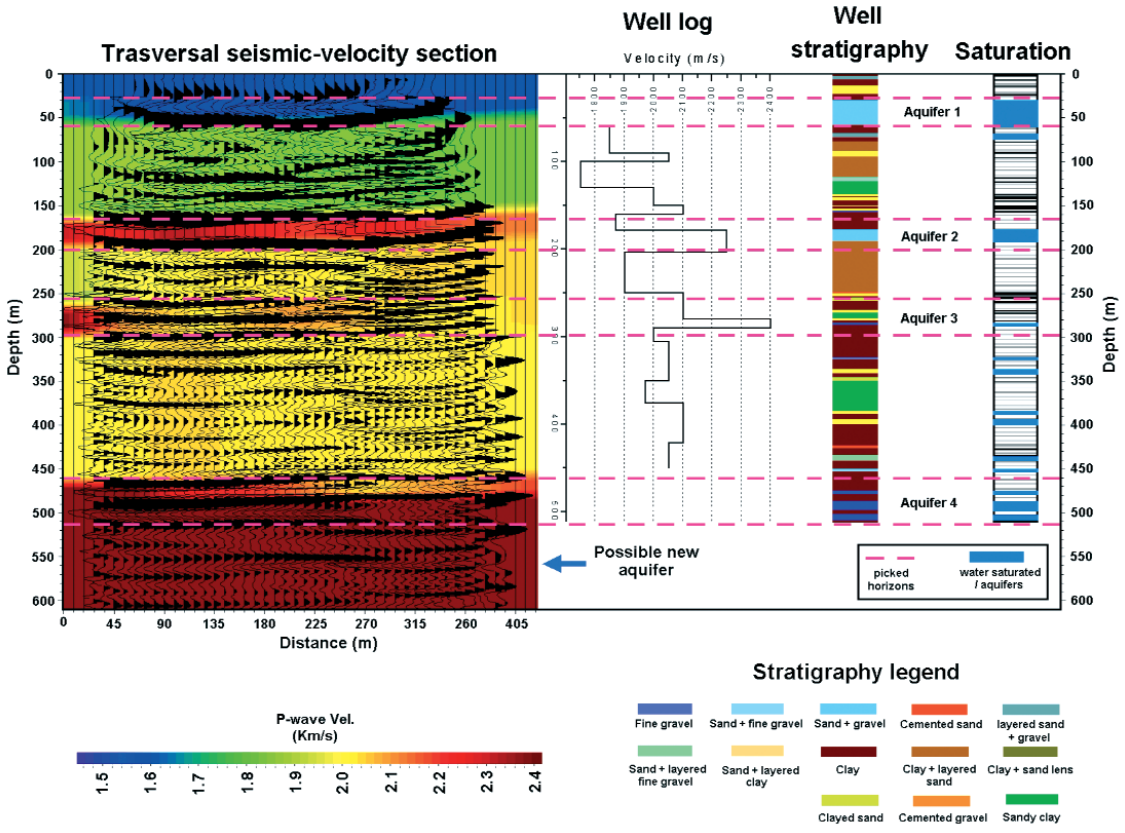

Fig. 9 - Correlation of the well stratigraphy with a transversal section of the small 3D July cubes. The velocity section is overlapped on the seismic migrated section. The dashed violet lines identify the picked horizons on the depth seismic section.

down-hole velocity log and the interval velocity section for aquifers 2 and 3. The four aquifers indicated on the well stratigraphy are characterized by high interval velocity values.

Finally, we computed the difference between the July velocity model and the March velocity model. Figs. 10 and 11 show the difference in the P-wave velocity inside the four aquifers, respectively, for the small and large cubes. The values are plotted on rectangular horizontal surfaces where the seismic coverage is sufficiently high. Outside these ranges, the fold is too low and the velocity values are not reliable. As you can see, the difference in the P-wave velocity values is very low. Considering a velocity error of about 5%, the 3D velocity models obtained from the analysis of the data acquired in the two different seasons are the same. This is due to the fact that the sediments are fully water saturated in both seasons, and the P-wave velocity is not sensitive to overpressures.

5. Conclusions

An iterative modelling and imaging in depth procedure was applied to a 4D high-resolution

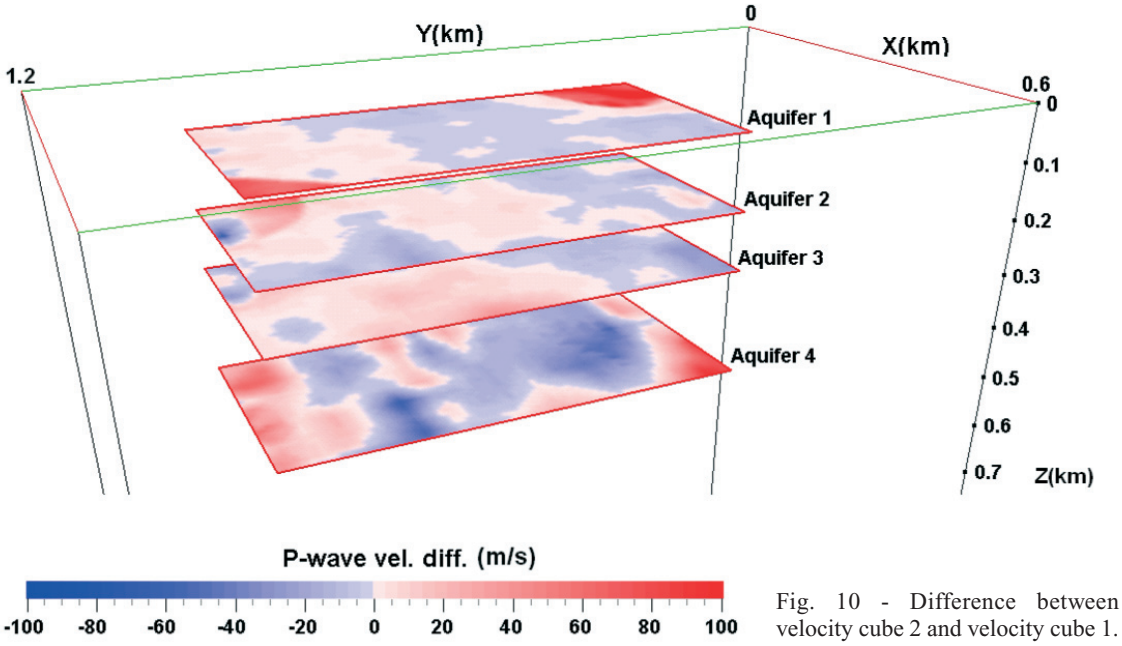

Fig. 10 - Difference between velocity cube 2 and velocity cube 1.

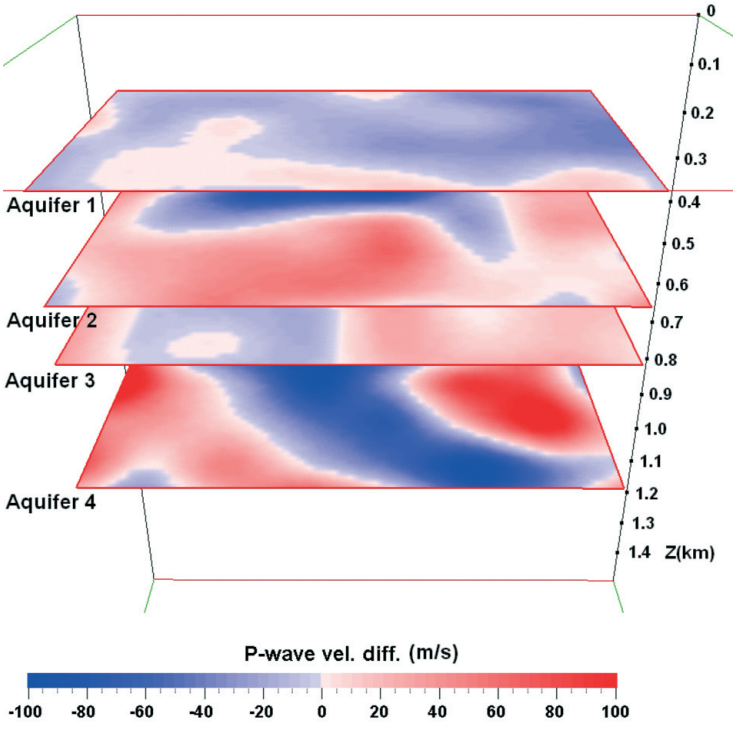

Fig. 11 - Difference between velocity cube4 and velocity cube 3.

seismic survey in order to study an important multilayered aquifer in an area of north-eastern of Italy with several catchment wells. Two interval velocity cubes and two migrated cubes were produced, corresponding to different periods (March and June). The 3D cubes detected the vertical sequence and the lateral variations of the layerswith high accuracy, so extending the well information to the surrounding area. This information is very useful, because it allows us to optimise the location of new wells, or to detect deeper sources, with a lower pollution hazard.

The more significant result of this work, which proves the effectiveness of the seismic method in aquifer exploration, is the discovery of two new deeper saturated layers at about 270 m and 480 m. In fact, a new 510 m deep well was drilled by the ABL at about 200 m from the seismic survey in order to verify the results of the seismic data analysis. There is a good correlation between the seismic sections and the well stratigraphy.

However, considering a velocity error of about 5%, the seismic method cannot detect any difference in the overpressure condition of the aquifers between the two periods. This conclusion arises also from a further work (Tinivella *et al*., 2009), where we used the velocity models to perform an AVO analysis in order to extract the porosity and the density maps of the main layers.

Acknowledgments. We are very grateful to Elvio Del Negro for his contribution and technical support in collecting the field data. We acknowledge the European Community that has supported this project (LIFE Project Number - LIFE04 ENV/IT/000500). We wish to thank the Acquedotto Basso Livenza, and in particular Enrico Marin, for the logistical support and all the information provided (hydrogeological data and the stratigraphies of the catchment wells).

REFERENCES

Giustiniani M., Accaino F., Del Negro E., Picotti S. and Tinivella U.; 2009: *Characterisation of shallow aquifers by 2D high-resolution seismic data analysis.* Boll. Geof. Teor. Appl., **50**, 29-38.

Rossi G., Dal Moro G., Picotti S., Vesnaver A. and Vuan A.; 2001: *A 3D seismic survey for groundwater protection.* In: 71st Annual Internat. Mtg. Soc. Expl. Geophys., Expanded Abstracts, San Antonio, Texas, pp. 1333-1336.

Tinivella U., Accaino F., Giustiniani M. and Picotti S.; 2009: *Petro-physical characterization of shallow aquifers by using AVO and theoretical approaches.* Boll. Geof. Teor. Appl., **50**, 59-69.

Vesnaver A., Böhm G., Madrussani G., Petersen S. and Rossi G.; 1999: *Tomographic imaging by reflected and refracted arrivals at the North Sea.* Geophysics, **64**, 1852-1862.

Yilmaz O.; 2001: *Seismic data analysis: processing, inversion and interpretation of seismic data.* SEG, Tolsa, Oklahoma, 2027 pp.

Corresponding author: Stefano Picotti
Dipartimento di Geofisica della Litosfera
Istituto Nazionale Oceanografia e di Geofisica Sperimentale
Borgo Grotta Gigante 42c, 34010 Sgonico (Trieste), Italy
phone: + 39 040 2140295; fax: +39 040 327307; e-mail: spicotti@inogs.it